

## CHAPTER 6

### **MOLECULAR FLEXIBILITY AND ORIENTATIONAL STATISTICS: RAMAN STUDY OF 7OB AND 8 OOB**

#### **6.1 Introduction**

The anisotropic properties of most thermotropic liquid crystals are explained by assuming the molecules to be elongated rigid rods possessing cylindrical symmetry. In the uniaxial nematic phase of the liquid crystal, if the symmetry axis of any individual molecule is assumed to make an angle  $\theta$  with the macroscopic symmetry axis, the molecular ordering can be specified completely, in principle, if we know the molecular orientational distribution function<sup>1</sup>  $f(\cos \theta)$  given by

$$f(\cos \theta) = \sum_{L, \text{even}} \frac{2L+1}{2} \langle P_L(\cos \theta) \rangle P_L(\cos \theta), \quad (1)$$

where  $P_L(\cos \theta)$  are the  $L^{\text{th}}$  even order Legendre

polynomials. Here  $f(\cos \theta)$  is normalized and the angular brackets denote averaging over all the molecules in the medium. The coefficients  $\langle P_L(\cos \theta) \rangle$  are defined by

$$\langle P_L(\cos \theta) \rangle = \int_{-1}^{+1} P_L(\cos \theta) f(\cos \theta) d(\cos \theta) \quad (2)$$

and are treated as orientational order parameters.

Explicitly, the first three coefficients are

$$\begin{aligned} \langle P_0(\cos \theta) \rangle &= 1, \\ \langle P_2(\cos \theta) \rangle &= \frac{1}{2}(3 \langle \cos^2 \theta \rangle - 1), \\ \langle P_4(\cos \theta) \rangle &= \frac{1}{8}(35 \langle \cos^4 \theta \rangle - 30 \langle \cos^2 \theta \rangle + 3) \\ &\dots(3) \end{aligned}$$

An experimental determination of the orientational order parameters  $\langle P_2(\cos \theta) \rangle$  and  $\langle P_4(\cos \theta) \rangle$ , designated hereafter as  $\langle P_2 \rangle$  and  $\langle P_4 \rangle$ , is of considerable interest from the standpoint of the statistical theories of molecular ordering in liquid crystals.

The anisotropies in  $M_{ij}$ — microscopic and macroscopic properties of liquid crystals have been extensively studied in the past in order to determine the variation of  $\langle P_2 \rangle$ , both with temperature and molecular structure.<sup>2</sup> However, relatively little is known as yet about the behaviour of  $\langle P_4 \rangle$  in most liquid crystals. Recently, polarized Raman scattering has emerged as a powerful method for the simultaneous determination of the absolute values of both  $\langle P_2 \rangle$  and  $\langle P_4 \rangle$  in uniaxial liquid crystals.<sup>3-6</sup> The resonance Raman effect has also been employed<sup>7</sup> for the same purpose.

In Appendix A the theoretical background concerning the Raman measurements of  $\langle P_2 \rangle$  and  $\langle P_4 \rangle$  is summarized.

A passing result that has emerged from the Raman studies is that  $\langle P_4 \rangle$  could assume negative values in some cases, especially within a temperature range close to the nematic-isotropic transition. Although this

behaviour is yet to be reconciled with predictions based on mean field theories, some speculations were put forward regarding its possible origin.<sup>1</sup> In their earliest study, Jen et al<sup>5</sup> suggested that negative  $\langle P_4 \rangle$  values may be rationalized if the flexibility of mesogenic molecules is taken into account - a feature that is ignored in theoretical calculations which assume the molecules to be rigid rods. Since molecular flexibility is enhanced by increasing the alkyl end-chain length it is of interest to examine the behaviour of  $\langle P_4 \rangle$  in closely related or homologous mesogens in order to assess the influence of molecular structure on this order parameter. With this in view, we have employed Raman scattering for the study of the temperature variation of  $\langle P_2 \rangle$  and  $\langle P_4 \rangle$  in two structurally related cyanobiphenyl liquid crystals, viz., 7CB (4,4'-n-heptylcyanobiphenyl) and 8 CB (4,4'-n-octyloxycyanobiphenyl). For 7CB our  $\langle P_4 \rangle$  values are consistently lower than those determined

earlier by Heger.<sup>4</sup> A comparison of our  $\langle P_4 \rangle$  results for 7OB and 8 OCB with Miyano's data<sup>5</sup> on 5OB (4,4'-n-pentylcyanobiphenyl) suggests that molecular flexibility is an important factor that serves to lower  $\langle P_4 \rangle$  well below the predictions of mean field theories.

## 6.2 Experimental

The transition temperatures of 7OB and 8 OCB, synthesized in our laboratory, were determined from thermal microscopy. Their respective phase transitions upon heating are:

### 7OB

solid  $\longrightarrow$  nematic  $\xrightarrow{314.8 \text{ K}}$  isotropic

### 8 OCB

solid  $\xrightarrow{327.0\text{K}}$  smectic A  $\xrightarrow{340.0\text{K}}$  nematic  $\xrightarrow{355.1\text{K}}$  isotropic.

The nematic phase of 7OB and the smectic A phase of 8 OCB were both found to supercool substantially on slow

coating from their mesophases and this fact effectively increased the mesophase range of the liquid crystals.

The oriented liquid crystal samples,  $\sim 100 \mu\text{m}$  in thickness, were held between glass cover slips or polished fused quartz plates. Homogeneous alignment was achieved by oblique vacuum coating of a layer of silicon oxide on the inner surfaces of the windows. Homotropic alignment was obtained by evaporating on the surfaces a dilute solution of octyl trimethylammonium bromide in chloroform. Alignment of samples was checked using a polarizing microscope. The sample cell was embedded in a heated copper block (see figure 2.7, chapter 2) and its temperature could be maintained at any desired value to within  $\pm 0.2^\circ\text{C}$ .

Raman scattering experiments were performed in the backscattering geometry (see figure 2.2,

chapter 2). The spectra were excited by  $\sim 100$  mW at 632.8 nm from a He-Ne laser. The scattered radiation was dispersed by a double grating monochromator (see Figure 2.3, chapter 2) and detected by a cooled photomultiplier tube (RCA 8952) in conjunction with a photon counting system. The experimentally measured Raman depolarization ratios were corrected for the unequal response of the monochromator for the two different polarizations of the scattered radiation. The  $\langle P_2 \rangle$  values were also measured independently by the method of infrared dichroism,<sup>9</sup> employing unpolarized infrared radiation and homogeneously aligned samples of thickness  $\sim 20$   $\mu$ m between polished NaCl windows.

Other details of the equipment and experimental procedure employed in the Raman and infrared measurements have been described in chapter 2 and elsewhere.<sup>9</sup>

### 2.3 Results and Discussion

The molecular structures of 5CB, 7CB and 8 CB are shown in figure 6.1. It is reasonable to assume that in all three cases the molecular long axis coincides with the line joining the centres of the two benzene rings. The intramolecular vibration corresponding to the - C H N stretch band also lies along the same axis. Our Raman and infrared experiments utilized this strong, isolated band in the spectra of 7CB and 8 CB.

Figure 6.2 is a schematic representation of the experimental geometries employed in measurements of Raman depolarization ratios in the aligned liquid crystal samples. Figure 6.3 is representative of the Raman band profiles of the - C H N vibration mode of the molecules. From the integrated intensities under the Raman band profiles, we obtained the three depolarization ratios<sup>3,5</sup>  $R_1$ ,  $R_2$  and  $R_3$  in the liquid crystalline phases:



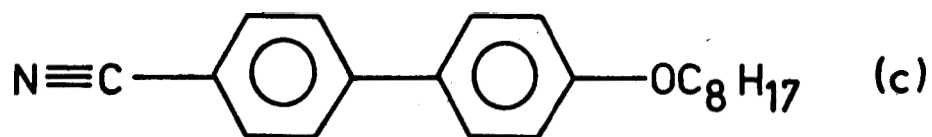
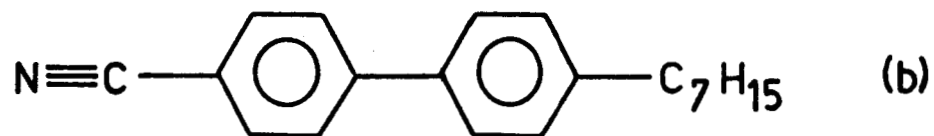
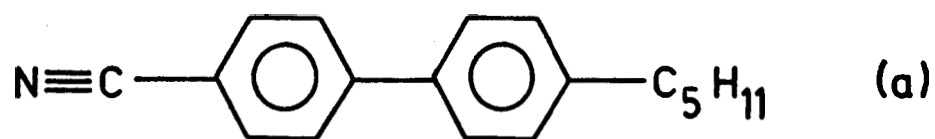


**FIGURE 6.1**

**Structures of 5CB, 7CB and 8 OCB molecules**

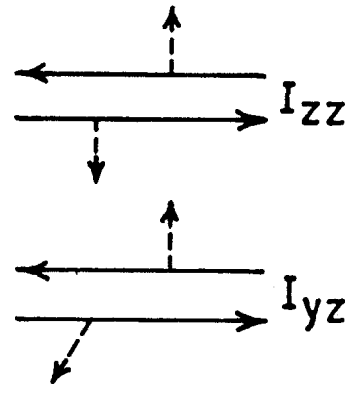
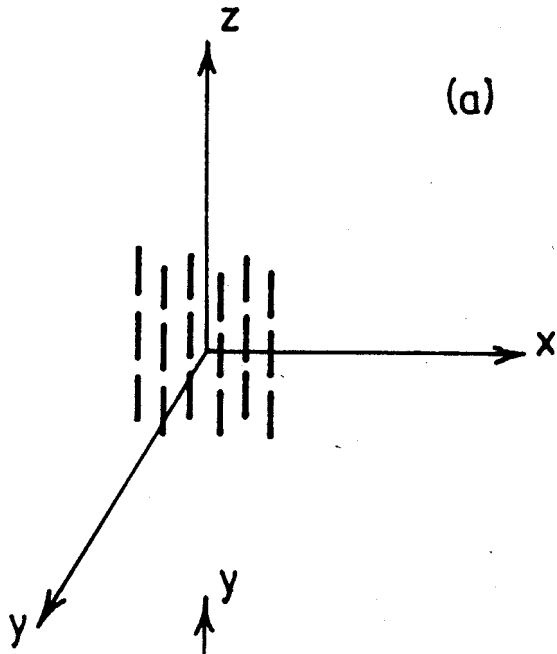
**FIGURE 6.2**

**Schematic representation of experimental geometries  
employed in measurements of Raman depolarization  
ratios in aligned liquid crystal samples.**

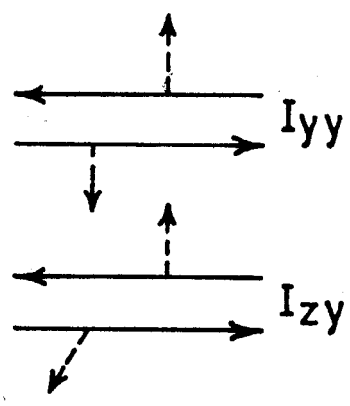
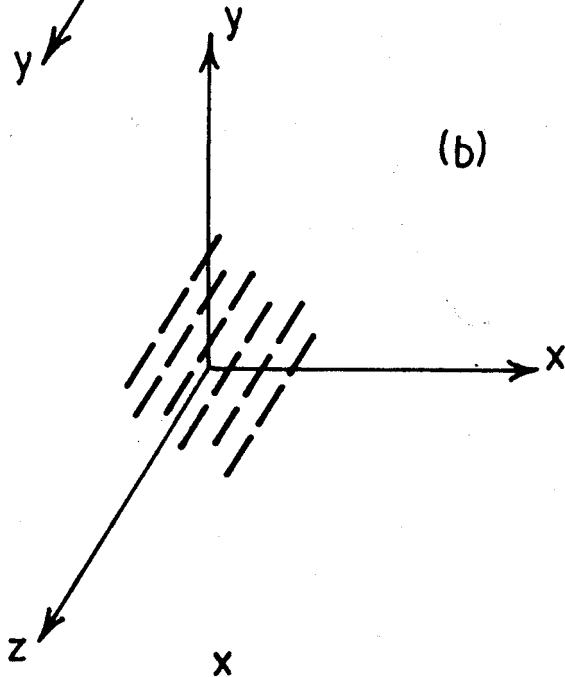
**(a) and (b) Homogeneous alignment**

**(c) Homeotropic alignment.**

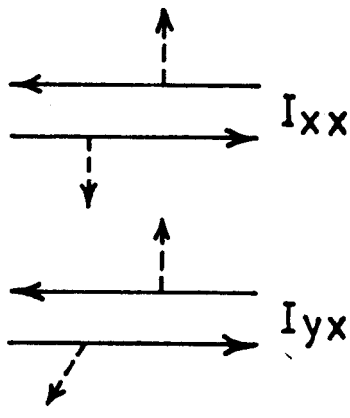
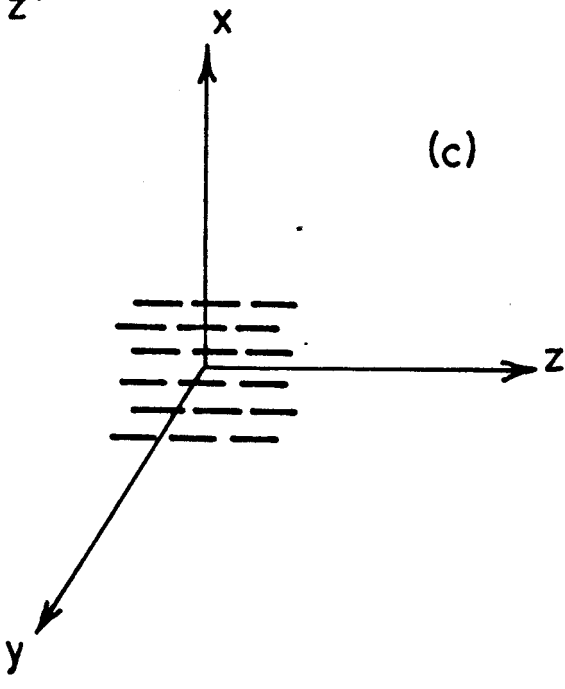
**Full arrows indicate the  $k$  vector of the radiation  
and the broken arrows show the polarisation. In  
each case the molecules are aligned in the  $z$ -direction.**



$$R_1 = \frac{I_{yz}}{I_{zz}}$$



$$R_2 = \frac{I_{zy}}{I_{yy}}$$



$$R_3 = \frac{I_{yx}}{I_{xx}}$$

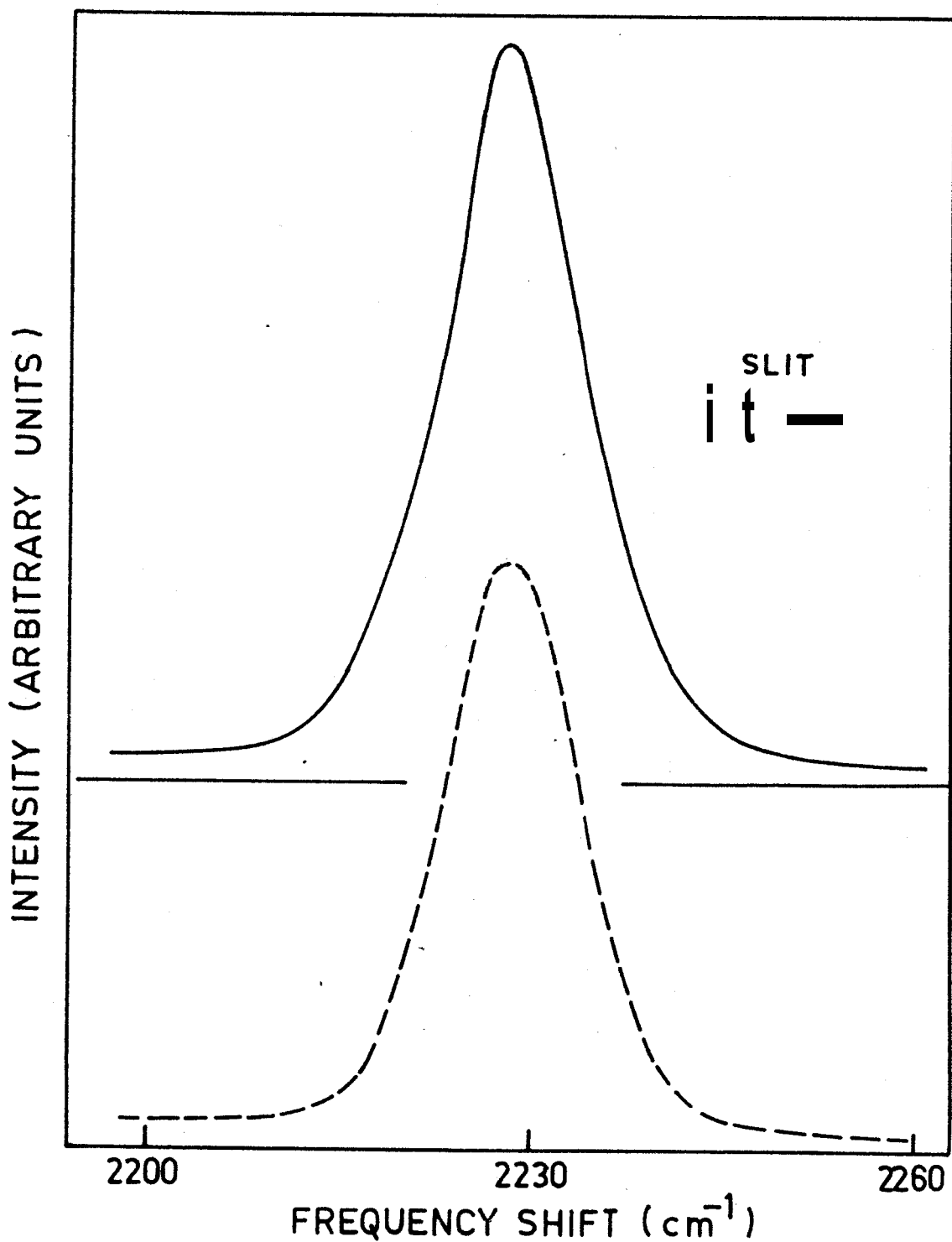


**FIGURE 6.3:** Raman band profiles of the  $-C \equiv N$  vibration mode of 70B in the isotropic phase. Full and broken curves correspond, respectively, to polarized and depolarized spectra.

$$R_1 = \frac{I_{YA}}{I_{AA}}, \quad R_2 = \frac{I_{MA}}{I_{MA}} \quad \text{and} \quad R_3 = \frac{I_{YA}}{I_{XX}}, \quad (4)$$

where the first subscript denotes the polarisation of the scattered light and the second refers to that of the incident light in the laboratory frame of axes  $(x, y, z)$ , the liquid crystal being aligned parallel to the  $z$ -axis (see figure 6.2). For the isotropic phase,  $R_{iso} = R_1 = R_2$ . For the liquid crystalline phases the observed depolarization ratios  $R_1$  and  $R_2$  were duly corrected for the effect of solid angle changes and transmission loss at the sample-cell interface.<sup>3, 10</sup> The corrected ratios are denoted by  $R_1/q_n$  and  $R_2/q_n$  where

$$q_n = \left( \frac{n_s + n_o}{n_s + n_e} \right)^2, \quad (5)$$

here  $n_s$  is the refractive index of the sample cell window material and  $n_o$  and  $n_e$  are, respectively, the ordinary and extraordinary refractive indices of the

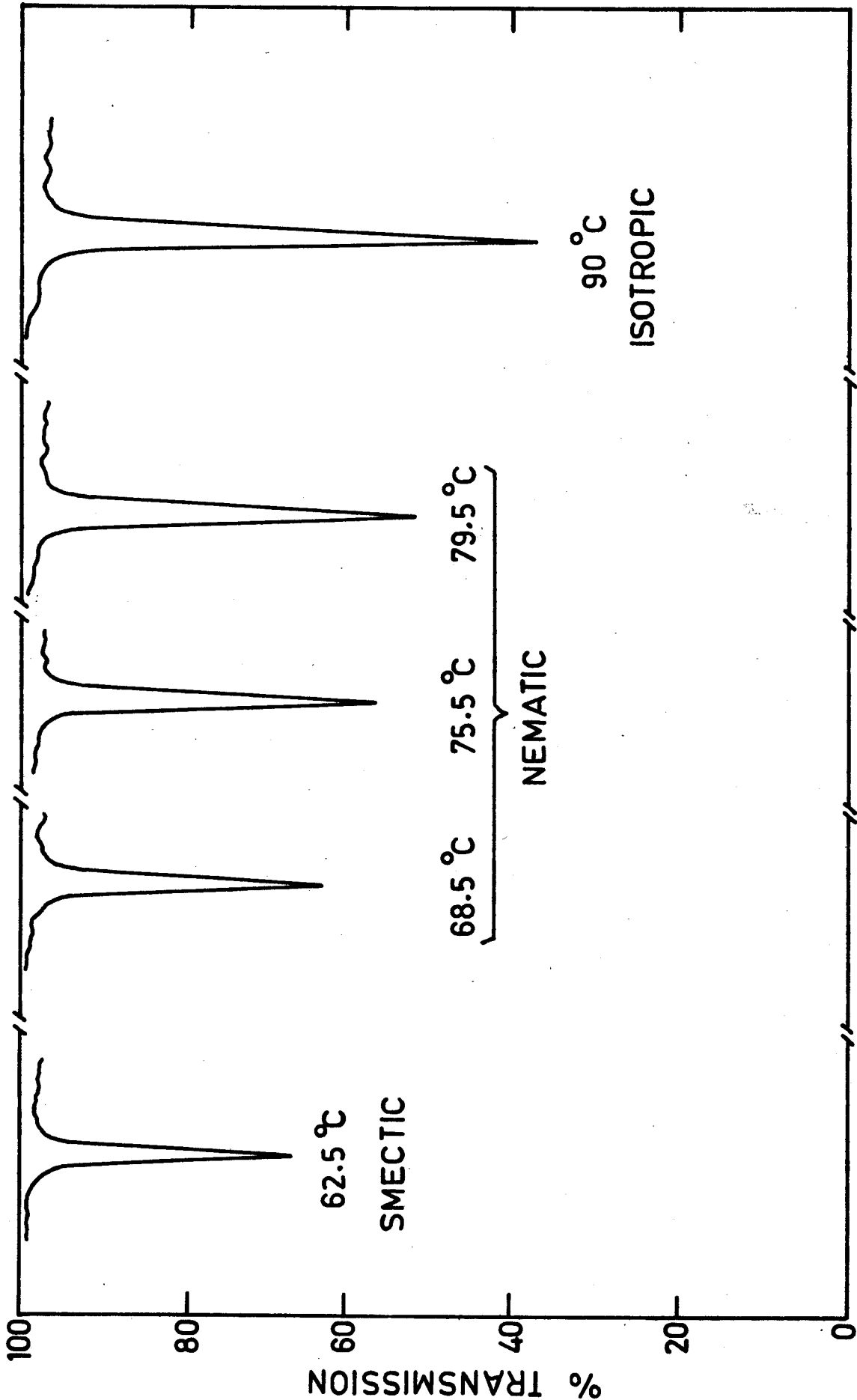
liquid crystalline sample. The pertinent refractive indices of 7CB and 8 CB were obtained by extrapolating the data of Karat and Madhusudana<sup>11</sup> to the Stokes-shifted wavelength ( $\sim 735$  nm) of the  $-C \equiv N$  Raman band. The final computations of  $\langle P_2 \rangle$  and  $\langle P_4 \rangle$  at each temperature was carried out following an iterative method, as outlined by Miyano.<sup>5</sup> Details of these calculations together with the computation program used are given in Appendix B.

The infrared absorption intensity of the  $-C \equiv N$  stretching mode of 8 CB in the liquid crystalline and isotropic phases is shown in figure 6.4. Similar results were obtained with 7CB. The liquid crystalline samples were homeotropically aligned. If  $R$  denotes the ratio of the integrated absorbance of this band in the homeotropically aligned mesophase to that in the isotropic phase, it can be shown that<sup>9</sup>

$$\langle P_2 \rangle = (1 - R) \quad (6)$$

FIGURE 6.4

Infrared absorption intensity of the  $\nu_{\text{C}=\text{O}}$  stretching mode of B OCB in smectic A, nematic and isotropic phases. The liquid crystalline samples were homeotropically aligned. The sample temperature corresponding to each trace is also shown. The peak occurs at  $\sim 2250 \text{ cm}^{-1}$ . The full width at half maximum intensity is  $\sim 12.5 \text{ cm}^{-1}$ .





The integrated absorbance was computed, with correction for the effects of finite spectral slit width, following Hammett's method.<sup>12</sup>

Figures 6.5 and 6.6 show the corrected Raman depolarization ratios versus temperature for the

liquid crystalline phases of 7OB and 8 OB. Their respective  $R_{100}$  values are 0.778 and 0.512. The

evaluated values of  $\langle P_2 \rangle$  as a function of temper-

ature from the Raman and infrared measurements are

shown in Figure 6.7 for both the mesogens. For compar-

ison, we have included the depolarization data of Karat and Hahnemann,<sup>11</sup> normalized to the  $\langle P_2 \rangle$

value obtained from our infrared measurements at the

mid-point of the nematic range. Good agreement is

seen between the  $\langle P_2 \rangle$  values derived from the Raman

and infrared measurements on the one hand, and the

depolarization data on the other.

The  $\langle P_4 \rangle$  results for 7OB and 8 OB are shown

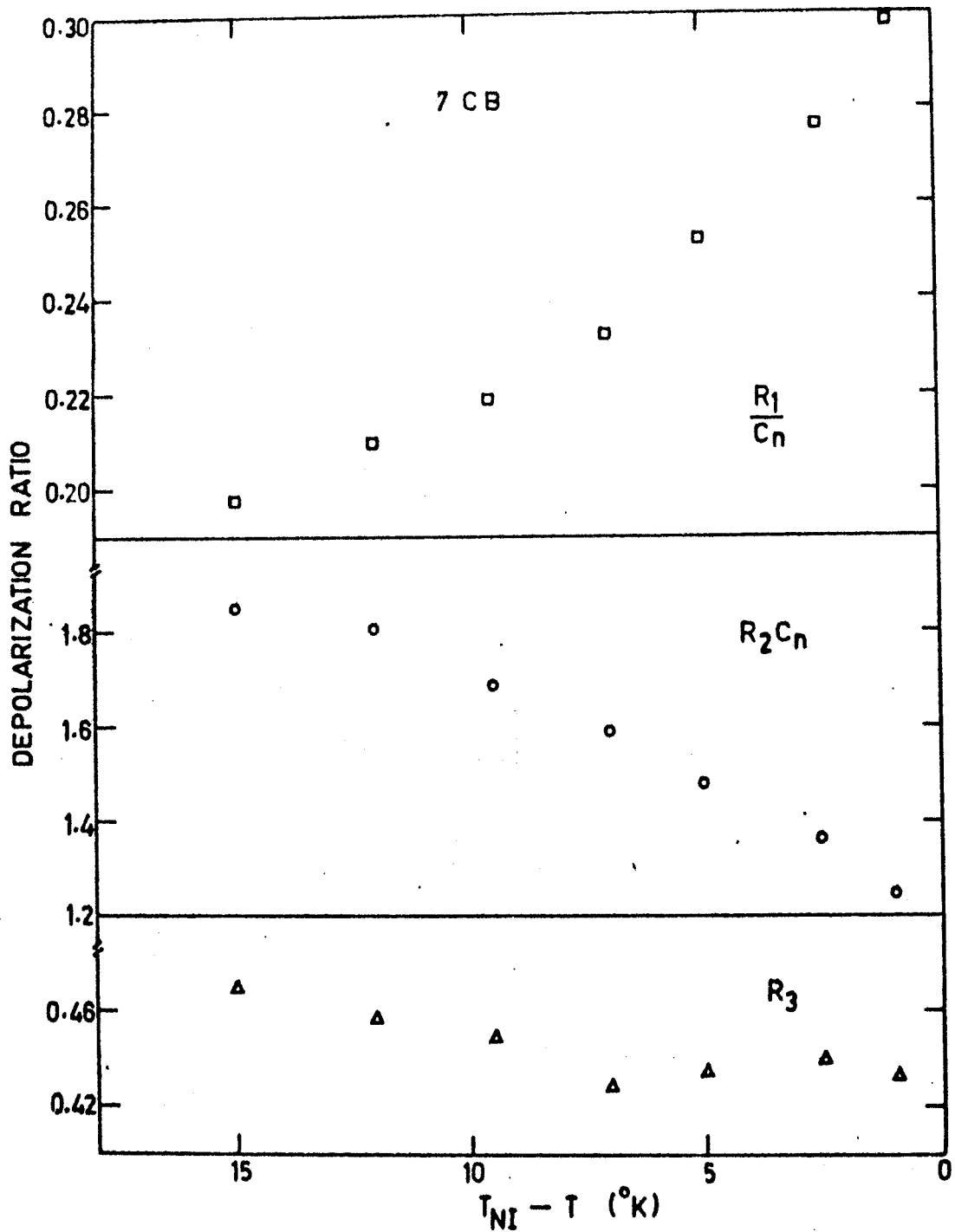


**FIGURE 6.5:** Corrected depolarization ratios of 7CB.

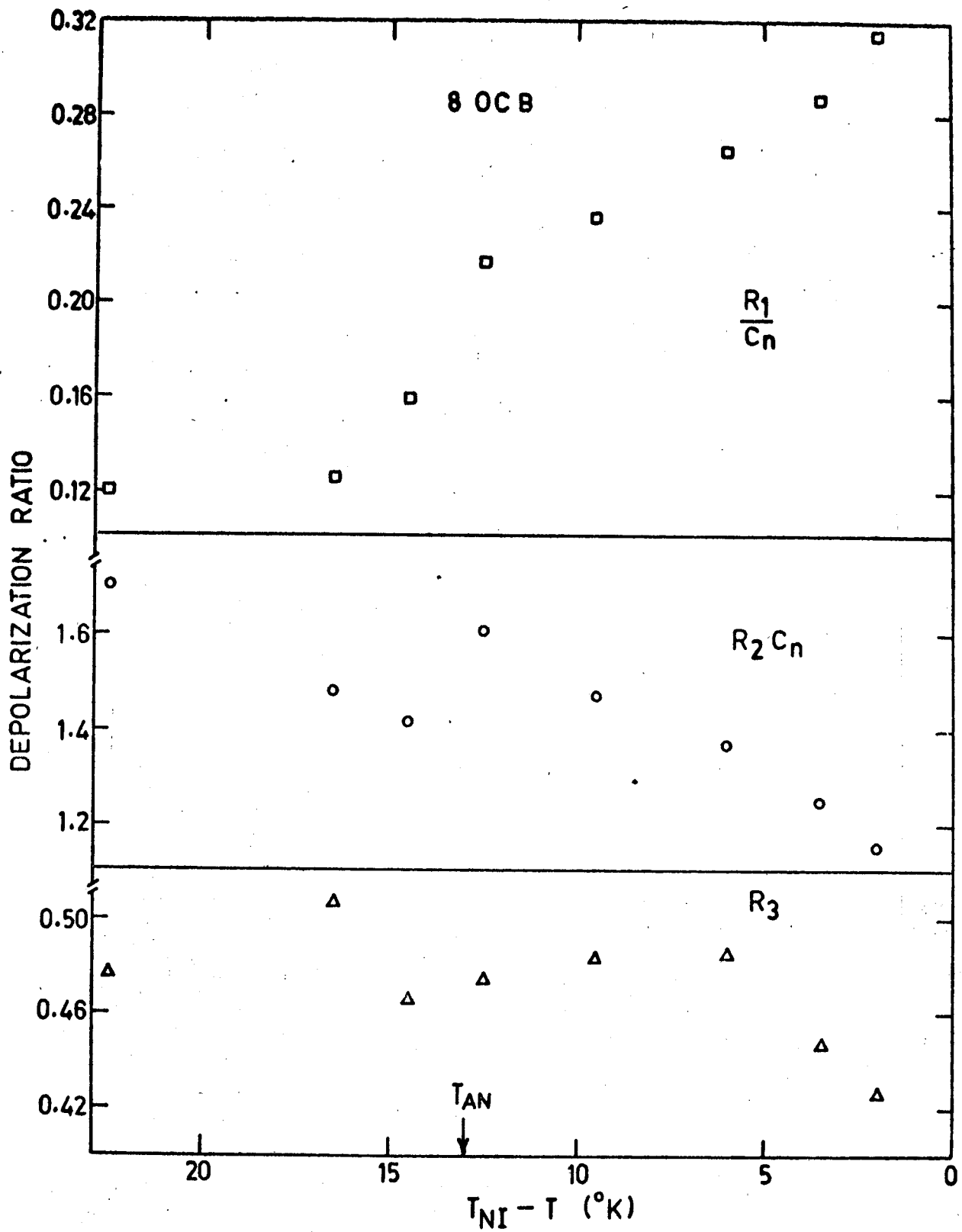


**FIGURE 6.6:** Corrected depolarization ratios of 8 OCB.  $T_{AN}$  is the smectic-nematic transition temperature.

**FIGURE 6.7**

Temperature dependence of  $\langle P_2(\cos \theta) \rangle$

in 7OB and 8 OCB.

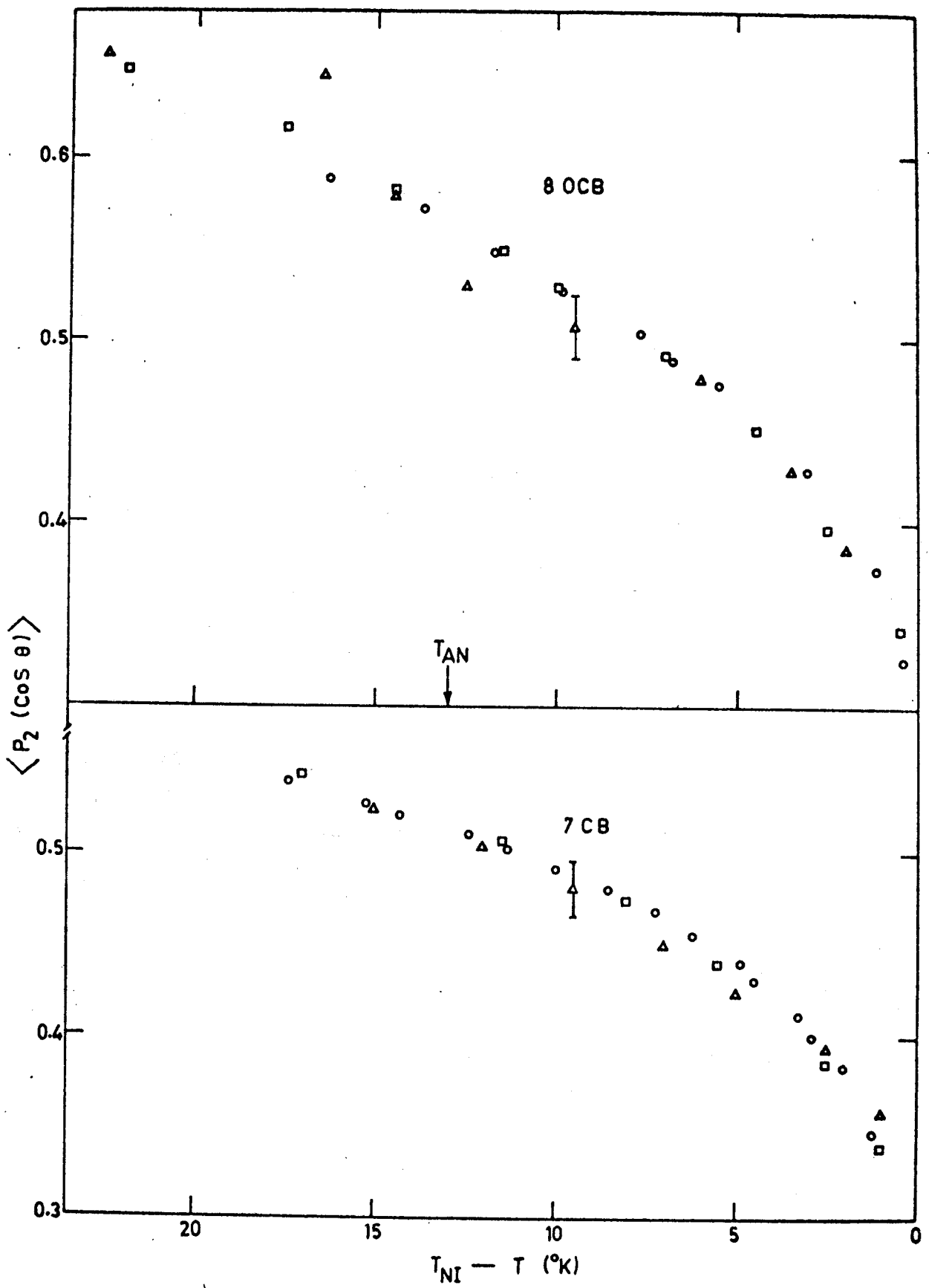
Triangles : Raman results

Squares : Infrared results

Circles : Birefringence data (Reference 11)

$T_{AN}$  is the smectic A - nematic transition

temperature of 8 OCB.



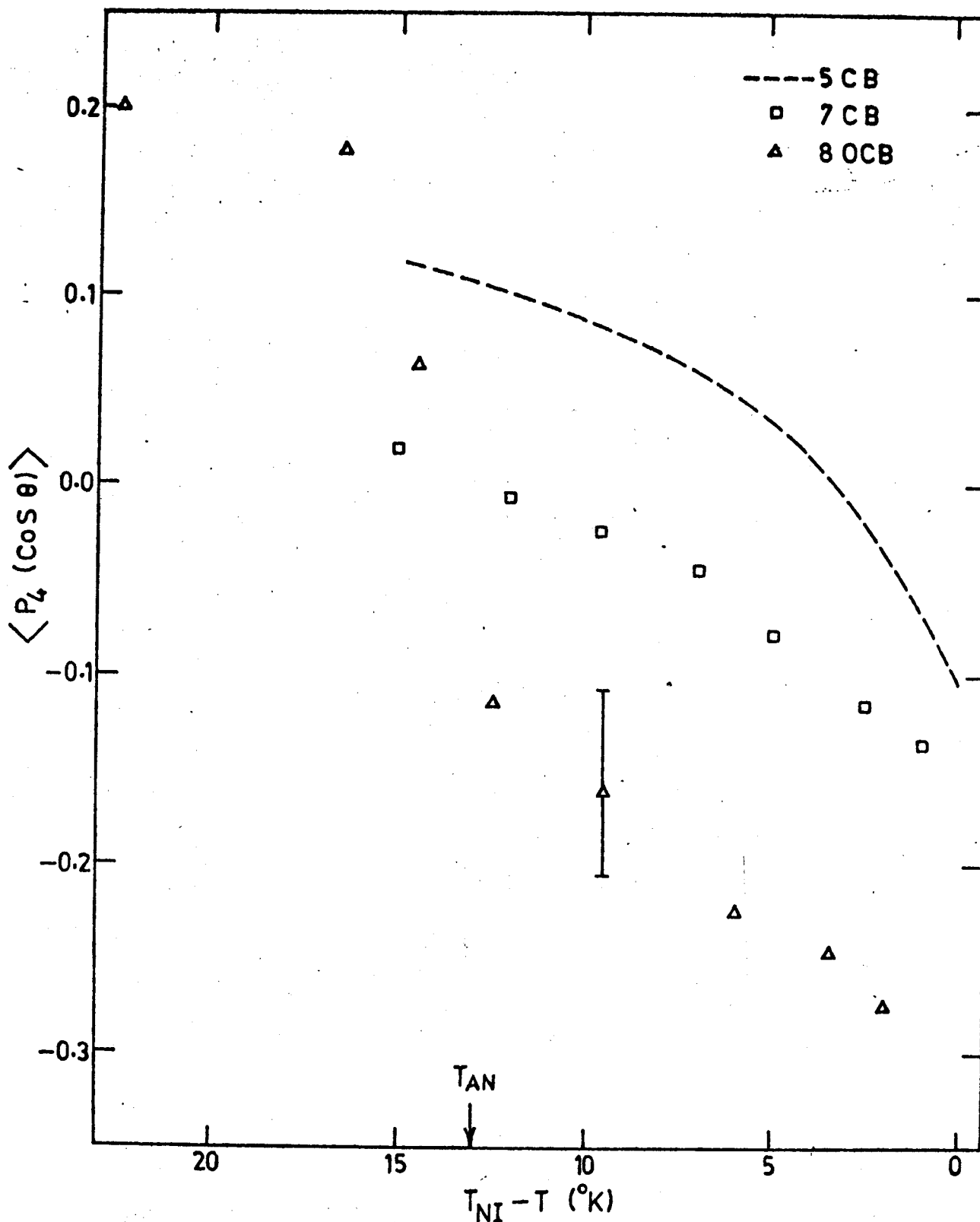


**FIGURE 6.8:** Temperature dependence of  $P_4(\cos \theta)$  in 5CB(Ref.5), 7CB and 8OCB.  $T_{AN}$  is the smectic A - nematic transition temperature of 8OCB.

in figure 6.8. Also shown here is the corresponding result obtained by Miyano<sup>5</sup> from a study of the  $-C \equiv N$  Raman band of 5OB. All three mesogens have identical cyanobiphenyl rigid cores, but differ in their end-chain length. Furthermore, flexible parts of the molecular end group are identical for both 8 OCB and 9 OB,  $imm \ C_9H_{17}$ . This is because, in 9OB the first methylene group which is linked to the phenyl ring is essentially immobile. To this extent, there is a further justification for intercomparing the data on 8 OCB, 7OB and 5OB. At any given relative temperature,  $(T_{NI} - T)$ , within the nematic range, these data show a decrease in  $\langle P_4 \rangle$  with an increase in end-chain

In view of the indicated experimental uncertainties in  $\langle P_4 \rangle$ , this observed trend is necessarily qualitative. The broken curve which depicts Miyano's results on 5OB is based on an extrapolation to zero sample thickness, while our data on 7OB and 8 OCB pertain to a sample thickness of  $\sim 100 \mu m$ . However,

the reported thickness dependence of the depolarization ratios is quite small<sup>5</sup> and the above conclusion would remain valid even if our data could be extrapolated to zero sample thickness.

From figures 6.7 and 6.8 we note that in the smectic A phase of 8 OCB both  $\langle P_2 \rangle$  and  $\langle P_4 \rangle$  register an increase. This reflects the greater degree of orientational order expected for this phase as compared to the nematic phase.

Our  $\langle P_4 \rangle$  results on 7CB differ from those reported earlier by Heger.<sup>4</sup> In the latter case, the estimated  $\langle P_4 \rangle$  values are all higher than those reported for 5CB even very close to  $T_{NI}$ . This is at variance with the trend seen in figure 6.8 with increasing chain length. Heger's  $\langle P_4 \rangle$  values were calculated under the assumption that the Raman tensor of the  $-C-H-N$  band is uniaxial within the molecular frame of reference.<sup>15</sup> Our calculated tensor parameters,  $a$  and  $b$  (see Appendix A), for 7CB and 8 OCB are shown in



tables 6.1 and 6.2, respectively. These results show that the relevant Raman tensor is biaxial for both cases, in accord with Miyano's data<sup>5</sup> on 5OB as well. We therefore feel that the above assumption coupled with the less straightforward experimental geometry adopted by Heger could have caused significant departures in his estimates of  $\langle P_4 \rangle$ . On the other hand, we note that Heger's  $\langle P_2 \rangle$  results are in reasonable agreement with ours. This is consistent with the fact that the experimental uncertainties associated with the Raman technique always cause a much smaller percentage error in  $\langle P_2 \rangle$  than in  $\langle P_4 \rangle$ .

Within a homologous series of liquid crystals,  $\langle P_2 \rangle$  is known to exhibit the well-known odd-even effect.<sup>14</sup> A similar effect is yet to be established in the case of  $\langle P_4 \rangle$  for any homologous series. We note, however, that the results in figure 6.8 are not complicated by any possible odd-even effect, in as much as 8 OB can be regarded as equivalent to 9OB with regard to the flexible part of

the molecule.

Any evaluation of  $\langle P_2 \rangle$  and  $\langle P_4 \rangle$  which relies on the optical or dielectric anisotropy of the medium must, in principle, include appropriate corrections for local field effects. A satisfactory theoretical estimate of these effects in liquid crystals remains as yet a difficult problem. However, based on other available empirical evidence Jen et al.<sup>3</sup> concluded that such corrections should not significantly alter the results obtained from the Raman technique. They attribute this to the notion that the short range correlations between molecules are essentially insensitive to temperature changes. We note that with the geometry adopted for our infrared measurements, possible local field corrections to  $\langle P_2 \rangle$  are expected to be well within 2%.<sup>9</sup> Thus, the agreement seen in figure 6.7 between the  $\langle P_2 \rangle$  results of both our Raman and infrared data indicates that the

necessary corrections to the Raman measurements are again well within the experimental uncertainties.

As pointed out earlier, the negative values of  $\langle P_4 \rangle$  obtained from Raman measurements are yet to be reconciled with the positive values predicted by mean field theories.<sup>1</sup> However, Jen et al.<sup>3</sup> have shown that there is nothing unphysical about negative values of  $\langle P_4 \rangle$ . They point out that negative  $\langle P_4 \rangle$  values would imply a stronger tendency on the part of the molecules to be tipped away from the director than predicted by the mean field theories. This tendency would be strongest near the nematic-isotropic transition temperature where  $\langle P_4 \rangle$  becomes most negative.

In conclusion, the present study demonstrates the influence of increasing end-chain length, and hence of molecular flexibility, on the order parameter  $\langle P_4 \rangle$ . It is of interest to extend these experiments to other mesogenic molecules which possess the same end alkyl

groups, but a more elongated rigid core structure.

In this context, a study of the corresponding homologues of 4,4'-n-alkylcyanoterphenyl series of liquid crystals would be especially relevant.

TABLE 6.1

Calculated Raman tensor parameters, a and b, of  
the  $-C \equiv N$  band of 7CB at different temperatures

---

$T_{HI} - T$ (K)	a	b
1.0	- 0.186	0.129
2.5	- 0.184	0.127
5.0	- 0.159	0.095
7.0	- 0.135	0.065
9.5	- 0.156	0.091
12.0	- 0.157	0.092
15.0	- 0.166	0.104

---

TABLE 6.2

Calculated Raman tensor parameters, a and b, of  
the  $\nu_{\text{C-H}}$  band of B CCB at different tempe-  
ratures

$T_{\text{HI}} - T$ (K)	a	b
2.0	- 0.240	0.319
3.5	- 0.239	0.318
6.0	- 0.248	0.333
9.5	- 0.227	0.298
12.5	- 0.204	0.260
14.5	- 0.186	0.232
16.5	- 0.185	0.231
22.5	- 0.156	0.188

References

- 1 E.B.Priestley and P.J.Wojtowicz, in Introduction to Liquid Crystals, ed. E.B.Priestley, P.J.Wojtowicz and P.Sheng (Plenum Press, New York, 1974).  
Chapters 3,4,and 6.
- 2 For a review, see P.G.de Gennes, The Physics of Liquid Crystals (Oxford University Press, London, 1974).
- 3 S. Jen, H.A.Clark, P.S.Pershan and E.B.Priestley, J.Chem.Phys. 66, 4635 (1977).
- 4 J.P.Heger, J.Phys. (Paris) Lett. 36, 209 (1975).
- 5 K.Miyano, J.Chem.Phys. 69, 4807 (1978).
- 6 L.P.G.Dalmolen and W.H.de Jeu, <sup>Ninth</sup> International  
Liquid Crystal Conference, Kyoto, 1980, paper B-4P.
- 7 H.Yoshida, Y.Nakajima, S.Kobinata and S. Maeda,  
Eighth International Liquid Crystal Conference,  
Kyoto, 1980, paper B-5P.

- 8 S. Jen, H.A.Clark, P.S.Pershan and E.B.Priestley,  
Phys. Rev. Lett. 31, 1552 (1973).
- 9 J.R.Fernandes and S.Venugopalan, J.Chem.Phys. 70,  
519 (1979); Mol.Cryst.Liquid Cryst. 35, 113 (1976).
- 10 M. Lax and D.F.Nelson, Phys.Rev. B4, 3694 (1971);  
see also, Proceedings of the Third Rochester  
Conference on Coherent and Quantum Optics,  
edited by L.Mandel and E.Wolf (Plenum Press, New York,  
1973) pp.415-445.
- 11 P.P.Karat and N.V.Madhusudana, Mol.Cryst.Liquid  
Cryst. 36, 51 (1976); Mol. Cryst. Liquid Cryst.  
47, 21 (1978); also see, P.P.Karat, Ph.D.Thesis,  
University of Mysore, 1977.
- 12 D.A.Ramsay, J.Amer.Chem.Soc. 74, 72 (1952).
- 13 J.P.Hegar, Ph.D.Thesis (Ecole Polytechnique Federale  
de Lausanne) 1976 (unpublished).
- 14 See, for example, S. Chandrasekhar, Liquid Crystals  
(Cambridge University Press, Cambridge, 1977) pp.51-54.